Pseudopotential description of rare earths in oxides: The case of Er2Si2O7

Lægsgaard, Jesper; Stokbro, Kurt

Published in:
Physical Review B Condensed Matter

Link to article, DOI:
10.1103/PhysRevB.63.075108

Publication date:
2001

Document Version
Publisher's PDF, also known as Version of record

Pseudopotential description of rare earths in oxides: The case of $Er_2Si_2O_7$

J. Lægsgaard[1] and K. Stokbro[2]
[1]*Research Center COM, Technical University of Denmark, Building 349, DK-2800 Kgs. Lyngby, Denmark*
[2]*Mikroelektronik Centret, Technical University of Denmark, Building 345 East, DK-2800 Kgs. Lyngby, Denmark*
(Received 27 June 2000; published 26 January 2001)

The applicability of ultrasoft pseudopotentials to the problem of rare-earth incorporation in silicates is investigated using the compound $Er_2Si_2O_7$ as a test case. It is found that density-functional theory within the generalized gradient approximation provides a good description of the structural parameters, when treating the Er $4f$ states as a partially occupied core shell. The density of states and the distribution of electronic charge are analyzed, and it is concluded that the presence of Er tends to increase the covalency of neighboring Si-O bonds.

DOI: 10.1103/PhysRevB.63.075108 PACS number(s): 61.50.Ah, 61.66.Fn, 71.15.Dx, 71.20.Ps

I. INTRODUCTION

Rare-earth incorporation in Si and SiO_2 hosts is becoming an increasingly important technique for creating advanced optical components. However, little is known about the microscopic structure around the rare-earth impurities and the mechanisms governing diffusion, clustering, etc. The materials have been investigated experimentally using a variety of techniques, including magnetic resonance,[1] extended x-ray-absorption fine structure,[2] optical spectroscopies[3] and more. However, as these experiments only give indirect information about impurity structures, there is a need to complement the experimental activities by theoretical calculations using accurate quantum-mechanical methods. A technique which recently proved useful in investigating the chemical structure of pure and doped silica is density-functional theory (DFT),[4,5] in combination with either norm-conserving or ultrasoft pseudopotentials.[6–15] These methods offer both accurate total energies and a computational efficiency which makes it possible to treat relatively large unit cells (containing 50–100 atoms) which is essential to describe the complex structural relaxations occuring in silica.

The inclusion of rare earths in pseudopotential calculations is complicated by the highly localized nature of the valence $4f$ orbitals, which makes it difficult to construct a soft pseudopotential giving a reliable description of these states. One solution to this problem is to neglect the relatively weak hybridization of the f states to the surrounding orbitals, treating them as a partially occupied core shell. The reasoning behind this idea is that the strong local Coulomb repulsion between electrons in a particular $4f$ multiplet suppresses the hybridization between the $4f$ orbitals and the other electronic states in the system, thus effectively eliminating the $4f$ contribution to the cohesive energy. It has been shown,[16] using the all-electron linear-muffin-tin-orbital method, that this procedure combined with intra-atomic energy corrections leads to a good description of rare-earth valencies, suggesting that the picture of localized $4f$ states is more realistic than that of itinerant $4f$-derived bands. A more sophisticated way of describing the f-electron states is the self-interaction corrected (SIC) DFT scheme,[17] in which the self-interaction present in the Hartree- and exchange-correlation terms of the DFT energy functional is explicitly subtracted. This has the effect of shifting the $4f$ level down in energy, which then supresses the interaction with the other valence states. It was recently demonstrated that SIC DFT provides an adequate description of the cohesive properties of rare-earth metals and sulfides.[18] The main advantage of the SIC method over the more primitive approach of treating the $4f$ orbitals as core states is that self-interaction correction allows for a unified description of differently occupied $4f$ states, and explicitly orthogonalizes the localized states to the extended valence states. However, for the systems of interest to us, the f occupancy (and hence the valence of the rare-earth ions) can easily be inferred from either the stoichiometry (in the case of crystalline systems) or from optical spectroscopy on the rare-earth f levels, and the orthogonalization is usually a minor concern, as the $4f$ levels in the rare earths are spatially well separated from the other valence orbitals.

In the present paper we construct an ultrasoft pseudopotential for Er, treating the Er $4f$ multiplet as a core shell, and test it by calculating the equilibrium volume and internal structure of the compound $Er_2Si_2O_7$, which is known from the crystallographic literature.[19] Furthermore, we analyze the electronic structure and charge distribution in the compound in order to test the assumptions made in the construction of the pseudopotential, and to shed light on the way in which the presence of Er influences the Si-O bonding.

The remainder of this paper is organized as follows: Sec. II briefly reviews the basic theory of Vanderbilts ultrasoft pseudopotential (US-PP) method,[20,21] and outlines our procedures for constructing Er pseudopotentials. In Sec. III our numerical results are presented and discussed. Section IV summarizes our conclusions.

II. THEORETICAL APPROACH

A. Elementary US-PP theory

It has recently been shown[22] that the US-PP scheme originally introduced by Vanderbilt[20] can be viewed as an approximation to the projector-augmented wave (PAW) all-electron method developed by Blöchl.[23] In this method, the wave function is expanded in a basis of plane waves augmented by atomic orbitals inside spheres centered around the ions in the lattice:

$$\Psi_{n\mathbf{k}} = \tilde{\Psi}_{n\mathbf{k}} + \sum_i \langle \tilde{\Psi}_{n\mathbf{k}} | \beta_i \rangle (\phi_i - \tilde{\phi}_i). \quad (1)$$

Here $\Psi_{n\mathbf{k}}$ is the true Kohn-Sham wave function, while $\tilde{\Psi}_{n\mathbf{k}}$ is a smooth pseudo-wave-function, that can be expanded in a limited number of plane waves. The functions ϕ_i and $\tilde{\phi}_i$ are atomic orbitals (i.e., a radial function times a spherical harmonic) centered on a particular site in the crystal, and are chosen to be identical outside the augmentation spheres, implying that $\Psi_{n\mathbf{k}}$ and $\tilde{\Psi}_{n\mathbf{k}}$ are also identical in this region. *i* is a combined orbital and site index. The ϕ_i functions are solutions of the all-electron Kohn-Sham equations[5] in the free atom, at chosen energies (usually the atomic eigenvalues are included), while the $\tilde{\phi}_i$ functions are soft pseudo-orbitals. The functions β_i are a set of duals to the pseudoorbitals, i.e.,

$$\langle \beta_j | \tilde{\phi}_i \rangle = \delta_{ij}. \quad (2)$$

Under the assumption of ''pseudocompleteness,'' by which we shall understand fulfillment, within the augmentation spheres of the requirement,

$$\tilde{\Psi}_{n\mathbf{k}} = \sum_i \langle \beta_i | \tilde{\Psi}_{n\mathbf{k}} \rangle \tilde{\phi}_i, \quad (3)$$

and, thereby,

$$\Psi_{n\mathbf{k}} = \sum_i \langle \beta_i | \tilde{\Psi}_{n\mathbf{k}} \rangle \phi_i, \quad (4)$$

the charge density may be written as[23]

$$n(\mathbf{r}) = \sum_{n\mathbf{k}} \left[\left| \tilde{\Psi}_{n\mathbf{k}}(\mathbf{r}) \right|^2 + \sum_{ij} \langle \tilde{\Psi}_{n\mathbf{k}} | \beta_i \rangle \langle \beta_j | \tilde{\Psi}_{n\mathbf{k}} \rangle Q_{ij}(\mathbf{r} - \boldsymbol{\tau}_i) \right], \quad (5)$$

$$Q_{ij}(\mathbf{r}) = \phi_i(\mathbf{r})^* \phi_j(\mathbf{r}) - \tilde{\phi}_i(\mathbf{r})^* \tilde{\phi}_j(\mathbf{r}). \quad (6)$$

$\boldsymbol{\tau}_i$ is the position vector of the augmentation sphere containing orbital *i* (we assume nonoverlapping spheres, so that the *ij* sum can be restricted to orbital pairs belonging to the same sphere). Usually only *spd* orbitals are included in the $\phi_i, \tilde{\phi}_i$ basis set. It can be shown that the incompleteness of the pseudo-orbitals arising from higher angular momentum components of $\tilde{\Psi}_{n\mathbf{k}}$ does not affect the spherical average of the charge density within the augmentation spheres.

In order for the pseudo-wave-functions $\tilde{\Psi}_{n\mathbf{k}}$ to be smooth, they must be solutions to a pseudo-Hamiltonian with a smooth potential term. To achieve this, the local potential from the ions, *V*, is replaced by a smooth local pseudopotential $\tilde{V}$ within some cutoff radius r_c^{loc}. Furthermore, the Q_{ij} functions defined above must be replaced by pseudized counterparts, $\tilde{Q}_{ij}$, to keep the Hartree and exchange correlation potentials smooth. A cutoff radius r_{in} is chosen, beyond which Q_{ij} and $\tilde{Q}_{ij}$ are identical. The pseudization is done in such a way that the lowest moments of the true and pseudo-electron densities are identical, in order to correctly describe the electrostatic interactions between the electronic density inside a given sphere and the density in the surrounding region. Introducing the pseudodensity $\tilde{n}$ as

$$\tilde{n}(\mathbf{r}) = \sum_{n\mathbf{k}} \left(\left| \tilde{\Psi}_{n\mathbf{k}}(\mathbf{r}) \right|^2 + \sum_{ij} \langle \tilde{\Psi}_{n\mathbf{k}} | \beta_i \rangle \langle \beta_j | \tilde{\Psi}_{n\mathbf{k}} \rangle \tilde{Q}_{ij}(\mathbf{r} - \boldsymbol{\tau}_i) \right), \quad (7)$$

the total energy within the framework of the DFT can now be written[22]

$$E_{DFT}[n, V] = E_{kin}[\{\tilde{\Psi}_{n\mathbf{k}}\}] + \int d\mathbf{r} \tilde{n}(\mathbf{r}) [\tilde{V}(\mathbf{r}) + \tfrac{1}{2} \tilde{V}_H(\mathbf{r})] + E_{xc}[\tilde{n}] + \sum_i \Delta E^i, \quad (8)$$

E_{DFT} being the DFT energy functional considered. $\tilde{V}_H$ is the Hartree potential arising from the pseudodensity, and ΔE^i is an energy correction term which only depends on the (real and pseudo) wave functions and charge densities within sphere *i*. Explicit expressions for ΔE^i within the PAW and US-PP formalisms are given in Refs. 21 and 22. While the correction terms in the PAW formalism are chosen so as to make the left-hand side of Eq. (8) exact, the corrections in the US-PP scheme are of an approximate nature, based on a linearization around the atomic occupation numbers.[22] However, in both formalisms it may be shown that the total energy functional is independent of $\tilde{V}$ under the assumption of pseudocompleteness. $\tilde{V}$ may therefore either be chosen to ensure optimal smoothness of $\tilde{\Psi}_{n\mathbf{k}}$, or to minimize the likely errors arising from violations of the pseudocompleteness requirement, e.g., by choosing $\tilde{V}$ to give correct scattering properties, at some chosen energy, in the lowest angular-momentum channel not included in the set of augmentation functions. In summary, the important parameters in the construction of ultrasoft pseudopotentials are the following:

(i) The radii of the augmentation spheres, which may be taken to be *l*-dependent. These are commonly denoted r_{cl}.

(ii) The pseudization radii for the local pseudopotential, r_c^{loc}, and the procedure for constructing this potential.

(iii) The eigenenergies used when solving the Schrödinger equation to obtain the functions ϕ_i, and the electron configuration assumed in the atomic all-electron calculation. The latter should resemble the distribution of electrons in the solid, but this may of course depend on the solid-state problem in question.

(iv) The pseudization radii for the *Q* functions. In the present work we shall use the same cutoff radius for all *Q* functions belonging to the Er atom.

Generally speaking, the choice of cutoff radii is a tradeoff between considerations of accuracy, which would favor radii as small as possible, since the electron density is described correctly beyond the pseudization spheres, and considerations of efficiency, which tend to favor larger spheres making the construction of smooth pseudo-wave-functions and pseudodensities easier. In addition, the spheres must be large enough that the core orbitals are well confined within them, in order to obtain a correct description of the charge density in the region intermediate between spheres.

B. Construction of Er pseudopotentials

The atomic configuration of Er is $4f^{12}5d^06s^2$. However, in a solid, a considerable *s*-*d* charge transfer must be expected, since the $5d$ and $6s$ shells are close in energy, and the degeneracy of the *d* shell is large. Furthermore, it is well known from optical spectroscopy that the $4f$-shell gives off an electron when Er is incorporated into a solid such as SiO_2. Therefore, it seems appropriate to base the pseudopotential construction on an atomic calculation with 11 electrons in the *f* shell (which is here treated as a partially occupied core state), and three electrons distributed over the valence states. Most of our trial pseudopotentials are based on the configuration $4f^{11}5d^26s^1$. Possible alternatives could be the ionic configuration $4f^{11}5d^16s^1$, which we have also investigated, or configurations with some of the electronic weight in the $6p$ orbitals.

For the local pseudopotential we have investigated two possible choices, requiring the potential to have correct scattering properties in either the *s* or *f* channel at an energy of 0.0 Ry relative to the vacuum level in the free-atom calculation (the eigenvalues of the atomic $5d$ and $6s$ states are -0.11 and -0.30 Ry, respectively). No reminiscence of the (unphysical) $4f$ resonance that would appear in a band calculation including the $4f$'s as valence states was seen with either choice, as will be discussed further below.

For the cutoff radii, we have chosen to put r_c^{loc} and all r_{cl}'s equal to 2.0 atomic units (a.u.), while the values of the *Q*-function pseudization radii were put to 1.0 a.u. in all channels. The nonlinear core correction introduced by Louie, Froyen, and Cohen[24] was applied within a radius of 1.2 a.u. With this choice of radii it was possible to construct pseudopotentials with solutions which were well-converged using a kinetic energy cutoff of $\sim$20 Ry for the plane-wave expansion. This is sufficient for the description of oxide systems since O US-PP's usually converge at 20–25 Ry. The confinement of the Er $5p$ orbital within r_c is, however, only $\sim$88%, while that of the $5s$ state is $\sim$96%. Therefore, these states must be included as valence states, which is quite possible without sacrificing the smoothness of the resulting potential. The only penalty is that more states, and more electrons, need to be included in the band calculations. For the study of Er impurities in large supercells, this is a minor concern. To avoid putting the $5sp$ states in the valence, one must go to a larger value of r_c, thereby reducing the reliability and transferability of the pseudopotential. To test the feasibility of this approach we constructed pseudopotentials with the $5sp$ states in the core using cutoff radii of 2.5 and 2.8 a.u. The number of atomic orbitals in the sp channels was taken to be equal to the number of valence shells (i.e., two when including the $5sp$ states in the valence, and one otherwise). The number of states in the *d* channel was always two: one calculated at the atomic eigenvalue, the other at an energy of 1.0 Ry relative to vacuum.

III. NUMERICAL RESULTS AND DISCUSSION

A. Lattice parameters for different pseudopotentials

The crystal structure of $Er_2Si_2O_7$ was determined by Smolin and Shepelev.[19] The crystal is monoclinic with space group $P2_1/b$, and a basis cell consisting of two formula units. The lengths of the Bravais vectors are $a=4.683$ Å, $b=5.556$ Å, and $c=10.79$ Å. The angle between vectors *a* and *b* is 96°, while *c* is orthogonal to both of the other vectors. Structural parameters are given in Table I. Whereas all Er atoms in the unit cell are equivalent, and similarly for Si, there are four distinct O species. Each Er atom in the structure is coordinated to six oxygen atoms of types 2, 3 and 4, as defined in Table I. The O(1) species is peculiar in that it is not coordinated to any Er atoms, but is instead bonded to two Si atoms with a bond angle of 180° (compare to $\sim$144° in α-quartz). The other three O species are each coordinated to one Si atom and two Er atoms, while all Si atoms are coordinated to four O atoms. A ball-and-stick model of the crystal structure is shown in Fig. 1.

TABLE I. Structural parameters for the inequivalent atoms in $Er_2Si_2O_7$. The position vectors are given as a linear combination of the *a*, *b*, and *c* Bravais lattice vectors described in the main text.

	Theory (PP1)			Experiment (Ref. 19)		
	τ_a	τ_b	τ_c	τ_a	τ_b	τ_c
Er	0.892	0.088	0.348	0.888	0.093	0.349
Si	0.360	0.643	0.388	0.360	0.644	0.387
O(1)	0.5	0.5	0.5	0.5	0.5	0.5
O(2)	0.203	0.864	0.450	0.205	0.865	0.449
O(3)	0.125	0.457	0.317	0.124	0.458	0.319
O(4)	0.620	0.751	0.298	0.618	0.752	0.298

To test our ultrasoft pseudopotentials, we have determined the theoretical equilibrium volume of the unit cell, allowing all internal coordinates to relax. A full optimization of the Bravais lattice parameters (the ratios b/a and c/a) and the angle between *a* and *b* was not attempted, but variations

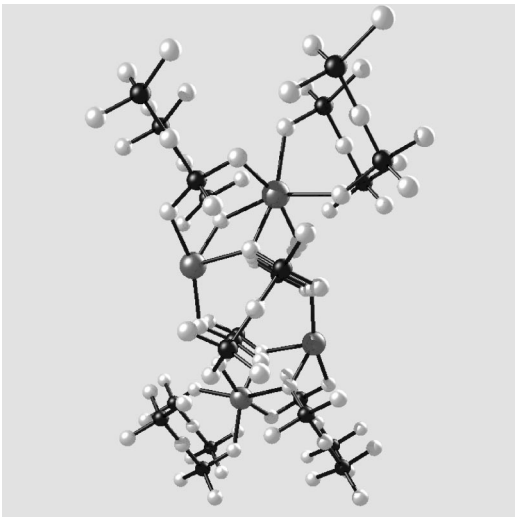

FIG. 1. Ball-and stick model of a part of the $Er_2Si_2O_7$ structure. Large grey spheres represent Er, small black spheres represent Si, and small white spheres represent O. All Er and Si atoms in the infinite crystal are equivalent. Note that some O atoms are 3 coordinated, and bonded to both Er and Si, while others are 2 coordinated and bond only to Si with a bond angle of 180°.

TABLE II. Theoretical equilibrium volumes and average Er-O and Si-O bond lengths for $Er_2Si_2O_7$ calculated with the pseudopotentials described in the main text.

Pseudopot.	PP1	PP2	PP3	PP4	PP5	PP6	Exp.
V_{WS} (Å^3)	288.0	287.3	289.5	279.2	282.6	289.0	279.1
$d^{av}_{Er\text{-}O}$ (Å)	2.278	2.276	2.284	2.245	2.259	2.282	2.262
$d^{av}_{Si\text{-}O}$ (Å)	1.642	1.642	1.644	1.642	1.643	1.644	1.621

of the individual parameters by 1% at fixed volume was found to raise the total energy in all cases, indicating that the optimized parameters would be quite close to the experimental ones. All calculations were performed using the generalized gradient approximation (GGA) by Perdew and Wang[25] (PW91) to the exchange-correlation part of the total energy. The plane-wave basis set was cut off at a kinetic energy of 25 Ry, and the Brillouin zone was sampled using two **k** points in the irreducible zone for the structural relaxations. For the density of states (DOS) calculations and charge-transfer analysis to be discussed below, a Monkhorts-Pack grid[26] consisting of 32 **k** points in the full zone was used. The results are shown in Table II, for six choices of pseudopotential: PP1 and PP2 were constructed from an atomic $5d^26s^1$ calculation, with the local pseudopotential chosen to scatter correctly in the s or f channel, respectively, at an energy of 0.0 Ry relative to vacuum. PP3 is similar to PP1, but is constructed from an atomic calculation in the ionic $5d^16s^1$ configuration. PP4 and PP5 treat the $5sp$ orbitals as core states, and have r_{cl}'s and r_c^{loc} at 2.5 (PP4) and 2.8 a.u. (PP5). In this case the local potential is chosen in a manner similar to PP2. PP6 is similar to PP2, but with cutoff radii as for PP4. It can be seen that the equilibrium volume of the unit cell is not very sensitive to the choice of the local pseudopotential, or the electronic configuration of the free atom. On the other hand, the inclusion of the $5sp$ states appears to be important for the construction of a reliable potential. Without these states, the equlibrium volume shows a considerably larger dependence on the sphere radius than is the case when putting the $5sp$'s in the valence (compare PP2 and PP6). Superficially, PP4 might seem the best choice, giving perfect reproduction of the equilibrium volume. However, an overestimation of the lattice constant by $\sim 1\%$ is quite common for the GGA approximation, and a closer look at the optimized structures indeed reveals that the agreement comes about through a distortion of the atomic coordinates: The Er-O bond lengths are underestimated, compared to experiment, while the Si-O bond lengths are overestimated. With $5sp$ states in the valence the bond lengths are consistently overestimated, so these potentials lead to more realistic atomic geometries. We have chosen to use PP1 for our further investigations, as the results with this potential seemed slightly less sensitive to the precise choice of scattering energy in the construction of the local potential, but for reasonable choices of this parameter PP2 would probably be an equally viable choice. The relative differences in the values of the logarithmic derivatives of all-electron (AE) and pseudo-wave-functions are shown in Fig. 2 for PP1 and PP2. It can be seen that the spd derivatives are very well reproduced in the pseudoatom, whereas there is a large deviation in the f channel because the bound $4f$ state appearing at $\sim$-8.3 eV in the AE atomic calculation is not accounted for in the pseudoatom. As we want to treat the $4f$ electrons as core states, this is of course the desired result. Note also that the derivatives for PP1 and PP2 are close to being identical, even for the f states.

The structural parameters calculated with PP1 are shown in Table I, and are seen to correlate well with the experimental ones. The lengths of the Er-O bonds vary between 2.25 and 2.31 Å in the theoretical calculation, whereas the experimental bond lengths lie between 2.23 and 2.31 Å. To test the transferability of the pseudopotential, an optimization of the lattice parameters of elemental Er was also performed. This is a quite stringent test of the present approach, as the couplings between a $4f$ shell and its surroundings are usually more important in metallic systems. Both theoretical calculations and analysis of experimental data indicated that Er also occurs in this case as a trivalent ion,[18,16] i.e., with 11 electrons in the $4f$ shell, consistent with our pseudopotential. Elemental Er crystallizes in a hexagonally close-packed structure, meaning that two lattice parameters, a and c/a must be determined. We performed the optimization using a plane-wave cutoff of 30 Ry and sampling the 1. Brillouin zone by a Monkhorts-Pack grid with eight divisions along each reciprocal-lattice vector. The theoretical lattice parameters were determined to be $a=3.56$ Å and $c/a=1.55$, in good agreement with the experimental values of $a=3.56$ Å and $c/a=1.57$. This result suggests that the present pseudopotential will offer a reliable description of most Er compounds, metallic as well as nonmetallic.

B. Electronic structure

To discuss the choice of atomic configuration for the pseudopotential construction in greater detail, we analyze the charge distribution arising in the solid-state calculation. The total charge inside a sphere of radius r_{cut} around some atom can be calculated in two ways: One can expand the augmented wave functions in atomic orbitals using Eq. (4), and obtain the density from those, or one can use the (plane-wave-expanded) soft density as calculated from Eq. (7). The latter approach is only valid beyond the Q-function pseudization radius r_{in}, because the pseudization of the Q functions does not preserve their shape but only their moments. On the other hand, the plane-wave-expanded density captures contributions from all angular-momentum components of the (pseudo-)wave-functions, while the use of Eq. (4) only captures the spd contribution. Thus a comparison of the results arising from each procedure constitutes a test of the ''pseudocompleteness'' assumption, i.e., the validity of Eqs. (3) and (4).

In Table III we give the valence charges inside the pseudization spheres of all inequivalent atoms in the $Er_2Si_2O_7$ lattice, and compare them to the charge of the free atom (in the $5d^26s^1$ configuration) within the same radius. The charge denoted AO is calculated from the atomic orbitals [that is, Eq. (4)], while the charge denoted PW is calculated from the (plane-wave-expanded) pseudodensity given by Eq. (7). The

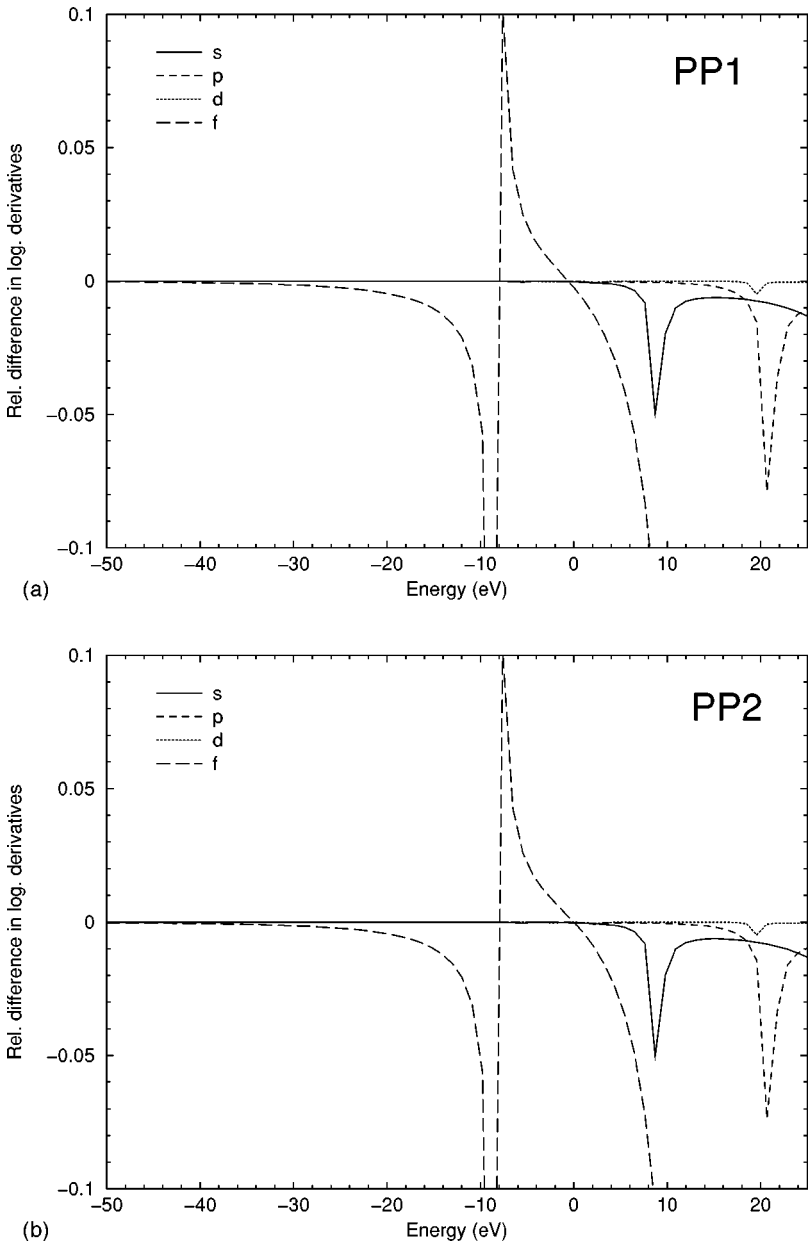

FIG. 2. The difference between logarithmic derivatives in the real atom and in the pseudo atom is plotted relative to the value in the real atom. In (a) results for PP1 are shown, while (b) gives the results for PP2. The energy is relative to the vacuum level.

charge is negative, as we only count the electronic charge (in units of e). The difference between the two methods of calculating the charge arise from corrections to Eq. (4) indicating incompleteness of the atomic pseudo-orbitals. For Er and O the two charges are in good agreement with each other, while there is a significant correction to the AO charge for Si. This is probably due to the fact that a substantial part of the charge within the rather large (1.9 a.u.) Si augmentation sphere comes from neighboring O orbitals, which will give rise to very asymmetric charge components in a coordinate system centered on the Si site. That this effect is not seen in the Er spheres may be due to the larger Er-O distance ($\sim$2.3 Å compared to $\sim$1.6 Å for Si-O).

TABLE III. Electronic charge within pseudization spheres for the inequivalent atoms in $Er_2Si_2O_7$. The sphere radii are 1.9 a.u. for Si, 1.3 a.u. for O, and 2.0 a.u. for Er.

	Free atom	Solid (AO)	Solid (PW)
Er	-7.85	-7.71	-7.70
Si	-1.40	-1.92	-2.04
O(1)	-3.96	-4.42	-4.41
O(2)	-3.96	-4.35	-4.35
O(3)	-3.96	-4.36	-4.36
O(4)	-3.96	-4.36	-4.36

The comparison between augmentation sphere charges in the solid and the free atom is interesting because the US-PP approximation to the PAW formalism is based upon a linear expansion of the density inside the augmentation spheres around the atomic occupation numbers. It can be seen from Table III that Er has a larger number of electrons inside the augmentation sphere in the free atom than in the solid. In Table IV, the AO charge is resolved on the different angular-

TABLE IV. Electronic charge within the augmentation sphere of Er, as calculated from Eq. (4) or in the free atom, resolved on different angular-momentum channels.

	s	*p*	*d*
Free atom	-1.98	-5.26	-0.61
Solid	-1.98	-5.42	-0.31

momentum components. The *s* occupations are seen to be identical, suggesting that $6s^1$ is an appropriate choice for the atomic configuration. The *d*-state occupation in the solid, on the other hand, is only half of that appearing in the free atom, with some of the charge being transferred to the *p* channel. However, the weight of the atomic $6p$ state within the augmentation sphere is only ~ 0.02, so the charge transfer to the *p* channel observed in the solid probably arises from states having both $5p$ and $6p$ components. Such a charge distribution cannot be modeled accurately in any atomic calculation. Table III also shows that the total charge inside the augmentation sphere is rather small, compared to the valency of 11, and if the charge around the atom is integrated out to a greater cutoff radius it turns out that there are in fact more electrons in the solid-state sphere than in the free atom (at 2.5 a.u., for instance, the difference is 0.87) due to contributions from the tails of neighboring atoms. Therefore, an atomic configuration such as $5d^16s^1$, with a positive net charge, may yield atomic orbitals of a wrong nature. If one wants to construct pseudopotentials tailored to a specific environment, a more fruitful procedure would probably be to go beyond the free-atom approach and use densities and orbital energies derived directly from a solid-state calculation.

As can be seen in Table III, the number of electrons in the Si augmentation spheres is larger in the solid than in the free atom. This may seem surprising, as the Si-O bonds are expected to have a partially ionic character, with charge being transferred from Si to O. However, since the atoms on the lattice will always overlap somewhat with the orbitals of the neighbors, whereas the free atom ''sees'' only its own charge, the result is to be expected. A better way of investigating the degree of ionicity of the bonds is to reference the charge around the different atoms to that arising from a superposition of unperturbed free-atom densities on the lattice in question, that is,

$$\rho_0(\mathbf{r}) = \sum_{\mathbf{R}} \sum_i \rho^i_{at}(\mathbf{r} - \mathbf{R} - \boldsymbol{\tau}_i). \tag{9}$$

Here $\mathbf{R}$ are the Bravais lattice vectors, while the *i* sum runs over the atoms of the unit cell, and $\boldsymbol{\tau}_i$ are the position vectors of the atoms in the cell with $\mathbf{R}=0$. In Table V we show the charge transfers calculated from this reference density, that is,

$$\Delta\rho = \int_{sphere} d\mathbf{r}[n(\mathbf{r}) - \rho_0(\mathbf{r})], \tag{10}$$

where the integral is evaluated over the augmentation sphere in question. The AE charge transfers are calculated with $n(\mathbf{r})$ determined from Eq. (4), while the PW values are derived replacing *n* with $\tilde{n}$ of Eq. (7). The values found for $Er_2Si_2O_7$ are compared to those found in α-quartz using similar calculational methods. In the rare-earth compound the transfer of electrons from Si is lower than in SiO_2, indicating an increased covalency of the Si-O bond. On the other hand, the transfer of electrons to O is similar in the two compounds, suggesting a saturation of the charge on the O atom. The decrease in the charge transfer from Si on going to the rare-earth compound then implies that charge transfer from Er to O is favored over charge transfer from Si to O. In a simple tight-binding picture, this finding may be rationalized by assuming that the Er *spd* levels lie above the Si *sp* levels. This would make the Er-O bond more ionic than the Si-O bond, and since the total charge transfer to O is similar in SiO_2 and $Er_2Si_2O_7$ this leaves less room for charge transfer from Si to O, i.e., the Si-O bond must assume a more covalent nature when the O atom is also bonded to Er. This interpretation is supported by an analysis of the electron DOS in $Er_2Si_2O_7$. In Fig. 3 we show the total DOS of this compound, together with its projections on the ϕ_i orbitals of Er, Si and O. It can be seen that the center of gravity of the Er-projected DOS is somewhat higher than that of the Si projection, implying that the Er levels in a tight-binding picture would be higher in energy than the Si levels. This conclusion is consistent with

TABLE V. Charge transfers within pseudization spheres for inequivalent atoms in $Er_2Si_2O_7$, referenced to either isolated free atoms or free-atom densities on a lattice [Eq. (9)]. Similar quantities for Si and O in α-quartz are also shown.

	Transfer rel. to free atom		Transfer rel. to lattice of free atoms	
	AO	PW	AO	PW
Er	0.14	0.15	0.28	0.29
Si	-0.51	-0.63	0.27	0.15
Si (α-quartz)	-0.41	-0.53	0.31	0.19
O(1)	-0.46	-0.46	-0.27	-0.26
O(2)	-0.40	-0.39	-0.25	-0.25
O(3)	-0.41	-0.40	-0.26	-0.25
O(4)	-0.41	-0.40	-0.26	-0.25
O (α-quartz)	-0.44	-0.43	-0.26	-0.25

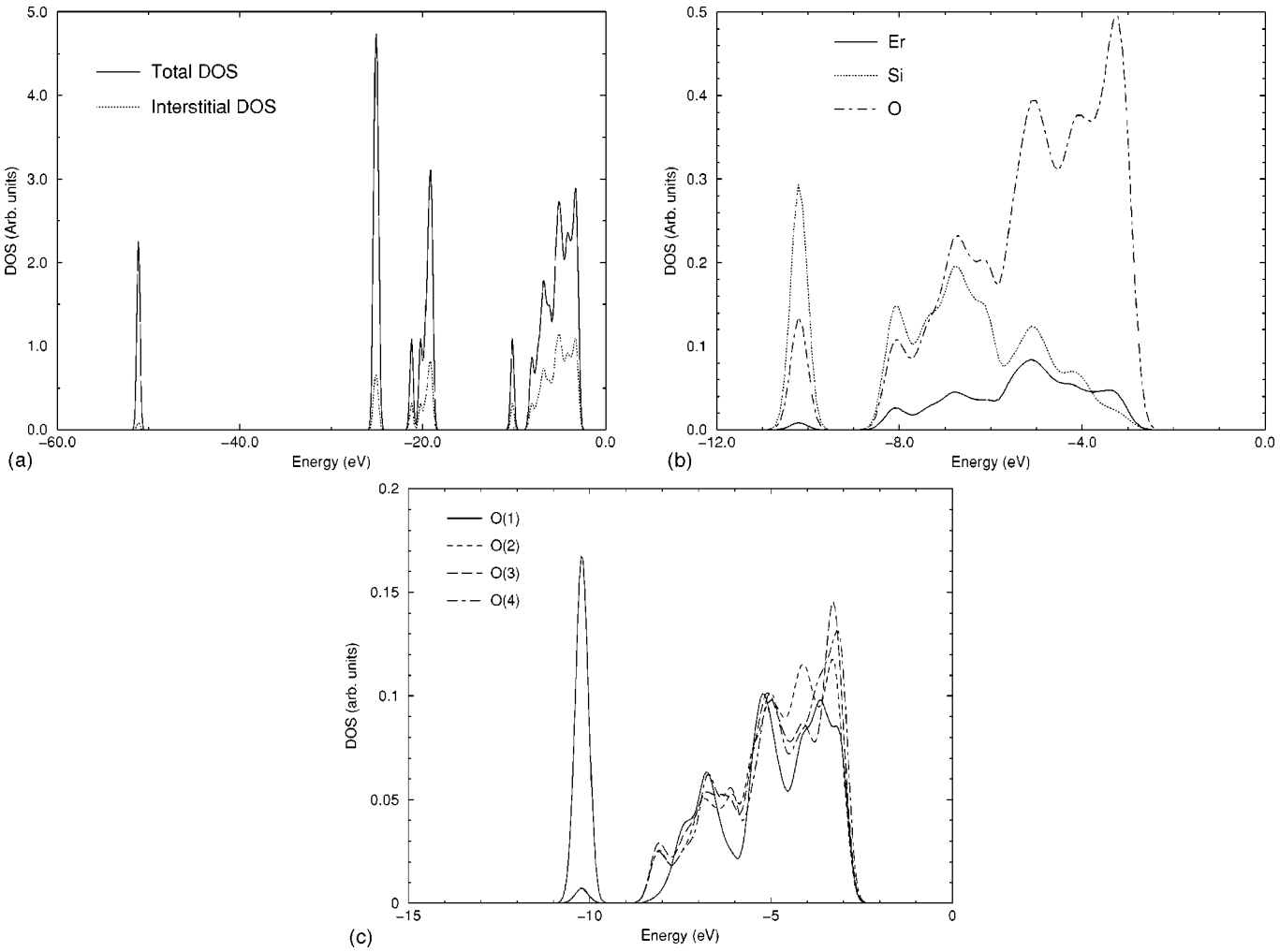

FIG. 3. Total (a) and orbital-projected DOS $Er_2Si_2O_7$. In (a) the contribution to the DOS from the interstitial region, obtained from subtracting the sum of ϕ_i-projected state densities from the total, is also shown. In (b) the projections on orbitals of different elements are shown for the uppermost valence states. The O DOS is summed over all positions, and scaled by a factor 4/14 to facilitate comparison. In (c) the DOS is resolved on the different inequivalent O atoms. The DOS was obtained sampling 32 points in the Brillouin zone with a Gaussian smearing of 0.25 eV. The Fermi level is at zero energy.

investigations of the oxidation of thin Er and Si layers on top of a SiO_2 film, showing that it is more favorable to oxidize Er than Si.[27]

In connection with the DOS it should also be noted that the split-off state appearing $\sim$10 eV below the Fermi level is primarily located on the O(1) atoms, which are not bonded to Er, and on Si. This is clear from Fig. 3(c), where the DOS has been resolved on different types of O atoms. That this state appears separated from the other Si-O states is yet another indication that the bonds between Si and the O atoms which are neighbors of Er are of a more covalent nature than the bonds to O atoms, which are only coordinated to Si. Finally, it should be noted that no state resembling an Er $4f$ resonance is seen in the DOS, confirming that this state is effectively excluded from the pseudopotential calculation.

IV. CONCLUSION

In conclusion, we have investigated the compound $Er_2Si_2O_7$ within the framework of density-functional theory using the ultrasoft pseudopotential approach. We find that the experimental equilibrium volume and internal structure are reasonably well described by the theory, provided that the Er $5sp$ semicore orbitals are included as valence states. The results thus demonstrate the feasibility of studying rare earths in oxide materials with pseudopotential methods. An analysis of the density of states and charge transfers indicate that the presence of Er reduces the ionic character of the Si-O bond in comparison with SiO_2.

ACKNOWLEDGMENTS

We thank Lars B. Hansen and the Center for Atomic-scale Materials Physics (CAMP) for valuable guidance on the use of their plane-wave band-structure program. Stimulating discussions with A. Svane are gratefully acknowledged. The use of Danish national computer resources was supported by the Danish Research Council.

[1] T. Fujiyama, T. Yokohama, T. Hori, and M. Sasaki, J. Non-Cryst. Solids **135**, 198 (1991); S. Sen and J. F. Stebbins, *ibid.* **188** (1995); M. Nogami, N. Hayakawa, N. Sugioka, and Y. Abe, J. Am. Ceram. Soc. **79**, 1257 (1996); K. Arai, S. Yamasaki, J. Isoya, and H. Namikawa, J. Non-Cryst. Solids **196**, 216 (1996).

[2] M. A. Marcus and A. Polman, J. Non-Cryst. Solids **136**, 260 (1991); P. M. Peters and S. N. Houde-Walter, Appl. Phys. Lett. **70**, 541 (1997); P. M. Peters and S. N. Houde-Walter, J. Non-Cryst. Solids **239**, 162 (1998); S. Sen, *ibid.* **261**, 226 (2000).

[3] K. Arai *et al.*, J. Appl. Phys. **59**, 3430 (1986); E. Delavaque *et al.*, IEEE Photonics Technol. Lett. **5**, 73 (1993); S. Tanabe and T. Hanada, J. Non-Cryst. Solids **196**, 101 (1996); M. Nogami and Y. Abe, *ibid.* **197**, 73 (1996); B. T. Stone and K. L. Bray, *ibid.* **197**, 136 (1996).

[4] P. Hohenberg and W. Kohn, Phys. Rev. B **136**, B864 (1964).

[5] W. Kohn and L. Sham, Phys. Rev. **140**, A1133 (1965).

[6] D. R. Hamann, Phys. Rev. Lett. **76**, 660 (1996).

[7] J. H. Th. Demuth, Y. Jeanvoine, and J. G. Angyan, J. Phys.: Condens. Matter **11**, 3833 (1999).

[8] A. Pasquarello and R. Car, Phys. Rev. Lett. **80**, 5145 (1998).

[9] M. Boero, A. Pasquarello, J. Sarnthein, and R. Car, Phys. Rev. Lett. **78**, 887 (1997).

[10] C. Carbonara, V. Fiorentini, and S. Massidda, J. Non-Cryst. Solids **221**, 89 (1997).

[11] A. Yokozawa and Y. Miyamoto, Appl. Phys. Lett. **73**, 1122 (1998).

[12] A. Oshiyama, Jpn. J. Appl. Phys. **37**, L232 (1998).

[13] N. Capron, S. Carniato, G. Boureau, and A. Pasturel, J. Non-Cryst. Solids **245**, 146 (1999).

[14] A. Continenza and A. D. Pomponio, Phys. Rev. B **54**, 13 687 (1996).

[15] J. Laegsgaard and K. Stokbro, Phys. Rev. B **61**, 12 590 (2000).

[16] A. Delin, L. Fast, B. Johansson, J. Wills, and O. Eriksson, Phys. Rev. Lett. **79**, 4637 (1997).

[17] J. P. Perdew and A. Zunger, Phys. Rev. B **23**, 5048 (1981).

[18] P. Strange, A. Svane, W. Temmerman, Z. Szotek, and H. Winter, Nature (London) **399**, 756 (1999).

[19] Y. Smolin and Y. Shepelev, Acta Crystallogr., Sect. B: Struct. Crystallogr. Cryst. Chem. **26**, 484 (1970).

[20] D. Vanderbilt, Phys. Rev. B **41**, 7892 (1990).

[21] K. Laasonen, A. Pasquarello, R. Car, C. Lee, and D. Vanderbilt, Phys. Rev. B **47**, 10 142 (1993).

[22] G. Kresse and D. Joubert, Phys. Rev. B **59**, 1758 (1999).

[23] P. Blöchl, Phys. Rev. B **50**, 17 953 (1994).

[24] S. Louie, S. Froyen, and M. Cohen, Phys. Rev. B **26**, 1738 (1982).

[25] J. Perdew, J. Chevary, S. Vosko, K. Jackson, M. Pederson, D. Singh, and C. Fiolhais, Phys. Rev. B **46**, 6671 (1992).

[26] H. Monkhorts and J. Pack, Phys. Rev. B **13**, 5188 (1976).

[27] S. Kennou, S. Ladas, M. Grimaldi, T. N. Tan, and J. Veuillen, Appl. Surf. Sci. **102**, 142 (1996).